IOP Publishing New J. Phys. 27 (2025) 064508 https://doi.org/10.1088/1367-2630/ade468

New Journal of Physics
The open access journal at the forefront of physics

Deutsche Physikalische Gesellschaft DPG
IOP Institute of Physics

Published in partnership with: Deutsche Physikalische Gesellschaft and the Institute of Physics

OPEN ACCESS

RECEIVED
19 December 2024

REVISED
9 April 2025

ACCEPTED FOR PUBLICATION
13 June 2025

PUBLISHED
23 June 2025

PAPER

Quantum steering transfer within quantum network

Xiao-Gang Fan[1,2], Jiaojiao Chen[1], Wei Xiong[3,4,*], Dong Wang[1] and Liu Ye[1,*]

[1] School of Physics and optoelectronics engineering, Anhui University, Hefei 230601, People's Republic of China
[2] Key Laboratory of Functional Materials and Devices for Informatics of Anhui Educational Institutions, Fuyang Normal University, Fuyang, Anhui 236037, People's Republic of China
[3] Department of Physics, Wenzhou University, Wenzhou 325035, People's Republic of China
[4] International Quantum Academy, Shenzhen 518048, People's Republic of China
[*] Authors to whom any correspondence should be addressed.

E-mail: xiongweiphys@wzu.edu.cn and yeliu@ahu.edu.cn

Keywords: quantum steering, adjustable measurements, quantum network

Abstract

Quantum steering is the ability that one system affects another one without delay by performing local measurements, which has garnered significant attention in the field of quantum information science. Here, we propose a linear network to realize tunable quantum steering with adjustable measurements. We show that forward steering of the first entangled source can be perfectly transferred to the state of two endpoints, regardless of measurements in the quantum network. However, for the backward steering between two endpoints, it displays a four-leaf clovers with rich symmetries with measurement parameters $\{\theta_j\}_{j=1}^{N-1}$ and is dependent on the parameters $\{\beta_j\}_{j=2}^{N}$ of the input state. By tuning the measurements far away from or close to the optimal values, one-way or two-way steering can be controllably realized. In addition, the error between the actual and optimal measurements is also taken into account in our proposal. The result indicates that a smaller error is beneficial for predicting two-way steering involving multiple measurements. Our proposal offers a promising way to realize the quantum steering transfer within linear networks.

1. Introduction

Quantum steering [1–4], a typical nonlocal correlation, is a crucial quantum resource in quantum information science [5]. Unlike other correlations such as quantum entanglement [6–9] and Bell nonlocality [10], it is intrinsic asymmetry [11–14], which leads to the birth of one-way steering [15, 16] and two-way steering. Due to this asymmetry, quantum steering has been widely investigated in semi-device-independent entanglement detection [17], one-sided device-independent quantum key distribution [18–20], randomness certification [21, 22], one-sided randomness generation [23], channel discrimination [24, 25], semi-device-independent and device-independent quantification of measurement incompatibility [26, 27], secret sharing [28–30], and secure quantum teleportation [31–33]. To characterize quantum steering, various steering criteria have been proposed, including linear steering inequalities [34–40], entropic uncertainty relations [41–43], correlation matrices [44, 45], steerable weight [46, 47], steering radius [48–50], critical radius [51, 52] and steering robustness [25]. Among these, the critical radius is an unconditionally sufficient and necessary steering criterion for two-party quantum states. This is due to the fact that critical radius provides a more stringent boundary between steering and unsteering, that is, critical radius can be used to detect all one-way and two-way steerable states from two-party states.

In addition, quantum steering, as well as quantum entanglement and Bell nonlocality, unveils rich structures in multiparty configurations, particularly within the context of quantum networks [53]. Specifically, the generation of quantum entanglement in initial networks is limited in range, which means that entangled states are established along the edges between adjacent nodes. This situation can be significantly improved via entanglement swapping operations, such as quantum repeaters [54], Bell state measurements [55–57], positive-operator-valued measurements (POVM) [58, 59], and quantum

channels [60, 61], on intermediate nodes [56]. Bej *et al* [58] investigated the generation of quantum correlations of the pair (1,4), encompassing quantum entanglement, three-measurement steering, and Bell nonlocality. This was achieved through the implementation of a POVM on the pair (2,3), whose process was starting from two independent Bell pairs (1,2) and (3,4). Similarly, Qi *et al* [59] conducted analogous research within a chain-type quantum network. Their results indicate that quantum correlations can be effectively controlled by manipulating the parameters of the POVM. In addition, the concept of network quantum steering based on network local hidden state models [62] has been proposed in a linear network consisting of trusted end points, intermediate untrusted parties, and fixed measurements on untrusted parties. This network is capable of remotely transmitting quantum entanglement and steering. However, achieving one-way or two-way steering between two remote qubits, along with the perfect transfer of steerability, remains a significant challenge within quantum networks, due to the limitations posed by currently existing sufficient and unnecessary steering criteria.

Motivated by this, we propose a linear quantum network involving adjustable projection measurements on intermediate parties, which is used to achieving steerability between two endpoints. Here, we use the sufficient and necessary steering criterion i.e. critical radius [51], to quantify the steerability. In our setup, forward steering, that is, the steerability of the first entangled source can be perfectly transferred to the steerability from the first qubit to the last one in a linear quantum network, which is independent of the number of the intermediate parties and the measurements. But for the backward steering, that is, the steerability from the last qubit to the first one in the network, its pattern versus measurement parameters displays a four-leaf clovers with aboundant symmetries, which can be tuned by the parameters $\{\beta_j\}_{j=2}^{N}$ of the input state. With increasing the measurements, we find that the translation symmetry is broken and tunable quantum steering, i.e. one-way or two-way steering, can be realized by adjusting the measurement parameters $\{\theta_j\}_{j=1}^{N-1}$ close to or far away from the optimal points $\left\{\theta_j^{\rm opt}\right\}_{j=1}^{N-1}$. By taking further into account the measurement error, we show that the network with multiple measurements tolerates small errors for non-vanishing backward steering. This indicates that tunable steerability can be engineered by controlling measurement errors. Our study provides a potential path to achieve tunable quantum steering and manipulate its direction in linear networks.

2. Model and critical radius

A quantum network, as shown in figure 1, comprises entangled sources of N pairs. Initially, we prepare the input state of the quantum network into a product state of all individual entangled sources, i.e. $\rho_{\rm in}=\otimes_{j=1}^{N}\rho_{A_jB_j}$. Then, we perform a sequence of joint measurements on all intermediate qubits. By tracing out all the intermediate qubits, the output state of the quantum network can be written as

$$\rho_{\rm out}=\frac{1}{P}{\rm Tr}_{B_1\cdots B_{N-1}A_2\cdots A_N}\left[\rho_{\rm in}\bigotimes_{j=1}^{N-1}M\left(\theta_j\right)\right], \tag{1}$$

where $P={\rm Tr}[\rho_{\rm in}\otimes_{j=1}^{N-1}M\left(\theta_j\right)]$ is the normalized factor and $M(\theta_j)=|\theta_j\rangle_{B_jA_{j+1}}\langle\theta_j|$ is jth joint measurement operator. The state $|\theta_j\rangle_{B_jA_{j+1}}=\cos\theta_j|00\rangle_{B_jA_{j+1}}+\sin\theta_j|11\rangle_{B_jA_{j+1}}$, with $\theta_j\neq k\pi/2\ \ (k=0,1,2,\ldots)$, is actually a Bell-like state. But when we set $\theta_j=(2k+1)\pi/4$, $|\theta_j\rangle_{B_jA_{j+1}}$ becomes the Bell state, and the corresponding joint measurement $M(\theta_j)$ reduces to the Bell state measurement.

Since our goal is to realize a one-way or two-way steering between two remote qubits (A_1 and B_N) in the proposed network, a critical radius [51] is introduced to quantify it. Specifically, for an arbitrary two-qubit state ρ_{XY}, the critical radius describing the steering from X to Y is defined as

$$R_{X\to Y}=\max_{\mu}\left\{\min_{O}\frac{\int_{\eta\in\mathcal{B}_Y}d\mu\left(\eta\right)\left|{\rm Tr}\left(O\eta\right)\right|}{\sqrt{2}\left\|{\rm Tr}_Y\left[\bar{\rho}_{XY}\left(I\otimes O\right)\right]\right\|}\right\}, \tag{2}$$

where $O=\frac{1}{2}\left(o_0I+\vec{o}\cdot\vec{\sigma}\right)$, with $\vec{\sigma}=\left(\sigma_x,\sigma_y,\sigma_z\right)$, is a single-qubit observable, μ is a distribution over states $\eta=\frac{1}{2}\left(I+\vec{v}\cdot\vec{\sigma}\right)$ in the Bloch ball $\mathcal{B}_Y$, and $\bar{\rho}_{XY}=\rho_{XY}-\frac{I}{2}\otimes\rho_Y$. Equation (2) indicates that the state ρ_{XY} is steerable from X to Y only when $R_{X\to Y}<1$. To further establish the region of the critical radius, we take a generized Bell diagonal state, i.e. $\rho_{\rm bds}=\frac{1}{4}\left(I\otimes I+t_x\sigma_x\otimes\sigma_x+t_y\sigma_y\otimes\sigma_y+t_z\sigma_z\otimes\sigma_z\right)$, as an example, but

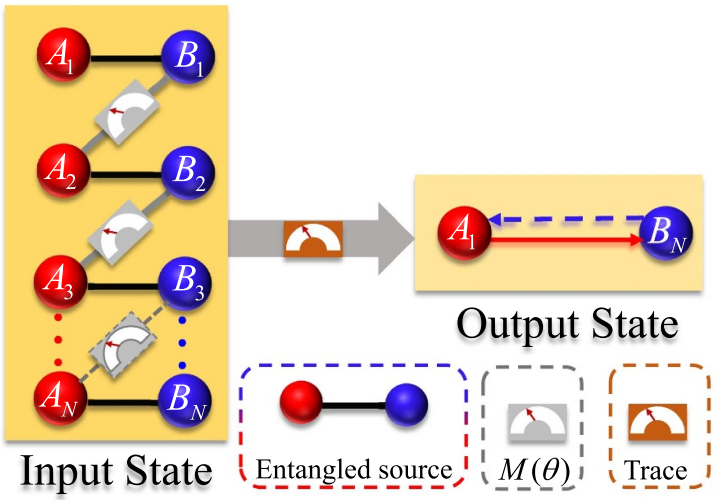

Figure 1. Schematic of the proposed quantum network. It consists of N-pair entangled sources, as the input state. The dial in gray denotes the joint measurement on all intermediate qubits, characterized by $M(\theta_j) = |\theta_j\rangle_{B_jA_{j+1}}\langle\theta_j|$ with $j = 1, 2, \ldots, N-1$. The dial in brown denotes the trace operation. The red (blue) arrow between two remote qubits (A_1 and B_N) means that A_1 (B_N) can steer the state of B_N (A_1), namely, forward (backward) steering.

without loss of generality to calculate it. By choosing the optimal observable and distribution,

$$R_{X\to Y}(\rho_{\text{bds}}) = \frac{2\pi\,|t_x t_y t_z|}{\int \left(t_x^{-2}n_x^2 + t_y^{-2}n_y^2 + t_z^{-2}n_z^2\right)^{-2} dS} \tag{3}$$

is obtained, where $n_x = \sin\alpha\cos\varphi$, $n_y = \sin\alpha\sin\varphi$, $n_z = \cos\alpha$, and $dS = \sin\alpha d\alpha d\varphi$. Equation (3) directly gives $R_{X\to Y} = 1/2$ for the Bell state ($t_x = -t_y = t_z = 1$) and $R_{X\to Y} \to \infty$ for the maximally mixed state($t_x = t_y = t_z = 0$), corresponding to the lower and upper limits of the critical radius. Therefore, the critical radius $R_{X\to Y}$ is limited to the region of $[1/2, \infty)$. This steerable zone can be in the region of $[0, 1]$ by redefining the critical radius,

$$\mathcal{R}_{X\to Y} = \max\left\{0, R_{X\to Y}^{-1} - 1\right\}, \tag{4}$$

which indicates that the state ρ_{XY} from X to Y is steerable when $\mathcal{R}_{X\to Y} > 0$, or equivalently $R_{\text{X}\to\text{Y}} < 1$.

3. Tunable steerability in quantum network

Next, we assume that parties A_1 and B_1 share an entangled Werner state ($p > 1/3$)

$$\rho_{A_1B_1} = p|\text{Bell}\rangle_{A_1B_1}\langle\text{Bell}| + (1-p)\frac{I_{A_1}}{2}\otimes\frac{I_{B_1}}{2}, \tag{5}$$

and other parties A_j and B_j are in an entangled pure state

$$\rho_{A_jB_j} = |\beta_j\rangle_{A_jB_j}\langle\beta_j| \quad \text{with} \quad j = 2, 3, \ldots, N, \tag{6}$$

where $|\beta_j\rangle_{A_jB_j} = \cos\beta_j|00\rangle_{A_jB_j} + \sin\beta_j|11\rangle_{A_jB_j}$ and $|\text{Bell}\rangle_{A_1B_1} = |\pi/4\rangle_{A_1B_1}$. From equation (3), one can see that the critical radii of the state $\rho_{A_1B_1}$ from $A_1 \to B_1$ and $B_1 \to A_1$ are equal, that is, $R_{A_1\to B_1} = R_{B_1\to A_1} = (2p)^{-1}$. As a result, the state $\rho_{A_1B_1}$ is two-way (no-way) steerable for $p > 1/2$ ($p \leqslant 1/2$). The term 'no-way steerable' here refers to the quantum state being unsteerable in both directions. But for an entangled pure state $\rho_{A_jB_j}$ given by equation (6), it is obviously two-way steerable [37, 51]. This indicates that there is no steering between remote parties A_1 and B_N without additional operations. In other words, a set of joint measurements is required to establish the steerability between these two parities. Taking advantage of the critical radius, we demonstrate that the steering direction between two remote parties (A_1 and B_N) can be changed by adjusting the measurement parameters $\{\theta_j\}_{j=1}^{N-1}$. For further clarity, we include a detailed investigation of the following examples.

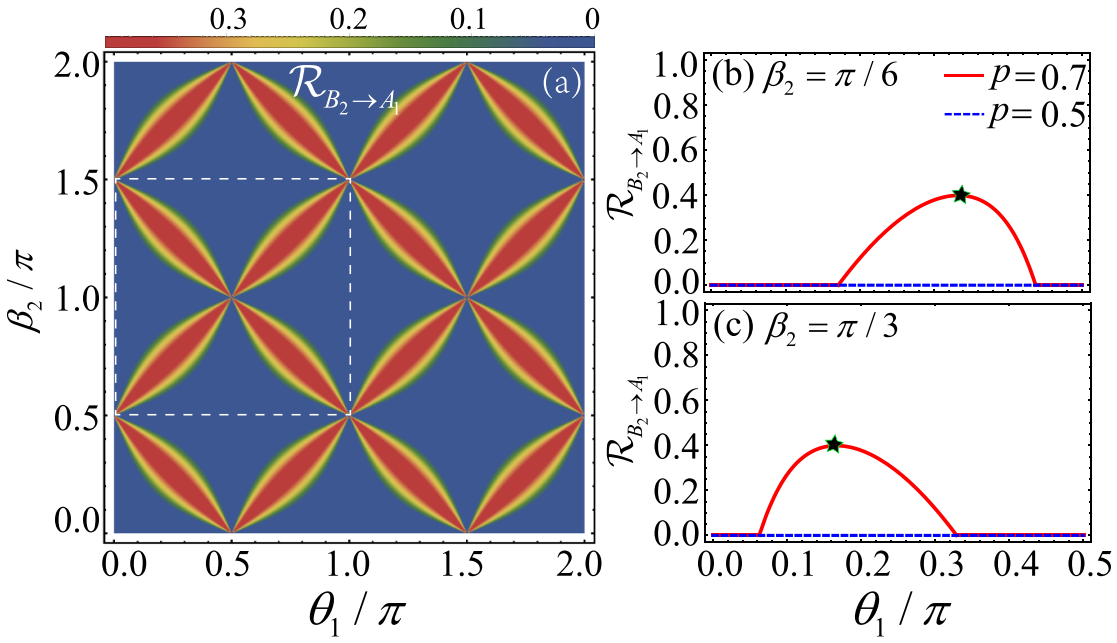

Figure 2. Backward steering ($\mathcal{R}_{B_2\to A_1}$) in a 2-pair entangled sources network versus the measurement parameter θ_1 and the parameter β_2 of the second entangled source. (a) $p=0.7$, (b) $\beta_2=\pi/6$ and (c) $\beta_2=\pi/3$. And in (b) and (c), $p=0.5$ and $p=0.7$ are considered.

3.1. Two entangled sources

We first show how to realize one-way and two-way steering between two parites (A_1 and B_2) in the simplest network, consisting of two entangled sources, i.e. $N=2$. In this case, only one joint measurement $M(\theta_1)$ is imposed. For a given input state (see equations (5) and (6)), the output state is (see details in appendix A)

$$\rho^{\text{out}}_{A_1B_2}=p\psi_{A_1B_2}+(1-p)\frac{I_{A_1}}{2}\otimes\psi_{B_2}, \tag{7}$$

where $\psi_{A_1B_2}=|g_2\rangle_{A_1B_2}\langle g_2|$ is an entangled pure state, and $\psi_{B_2}=\text{Tr}_{A_1}(\psi_{A_1B_2})$ is the reduced density matrix. In the above expressions, $|g_2\rangle_{A_1B_2}=\cos g_2|00\rangle_{A_1B_2}+\sin g_2|11\rangle_{A_1B_2}$, with the g-function

$$g_2=\frac{1}{2}\arccos\left(1-\frac{2}{1+\cot^2\beta_2\cot^2\theta_1}\right). \tag{8}$$

For the output state $\rho^{\text{out}}_{A_1B_2}$, its critical radius from A_1 to B_2 is $R_{A_1\to B_2}=(2p)^{-1}$ (see details in appendix B), which is the same as the critical radius of the input state $\rho_{A_1B_1}$ from A_1 to B_1. This means that the steerability of the state $\rho_{A_1B_1}$ from A_1 to B_1 can be perfectly transferred to the steerability of the state $\rho^{\text{out}}_{A_1B_2}$ from A_1 to B_2. For the critical radius $R_{B_2\to A_1}$ of the state $\rho^{\text{out}}_{A_1B_2}$, it can not be given analytically. Fortunately, it can be numerically investigated with equation (2) (see details in appendix B). To show the numerical result, we plot the redefining critical radius $\mathcal{R}_{B_2\to A_1}$ as functions of parameters θ_1 and β_2 in figure 2(a) with $p=0.7$. Intuitively, the pattern resembles *four-leaf clovers* having central-, axial-, rotational and translation-symmetry (see the dashed box), which can be attributed to the periodic nature of the cotangent function in equation (8). The leaf denotes the steerability from B_2 to A_1 of the output state, and the non-leaf part denotes no steerability from B_2 to A_1. Obviously, an optimal steering exists (see the pattern in red) and we can tune parameters θ_1 and β_2 to achieve it. For clarity, we further plot $\mathcal{R}_{B_2\to A_1}$ versus the parameter $\theta_1\in(0,\pi/2)$ with fixed $\beta_2=\pi/6$ and $\pi/3$ in figures 2(b) and (c), respectively. The unsteerable input state $\rho_{A_1B_1}$ with $p=1/2$ (see discussions after equation (6)) leads to the output state $\rho^{\text{out}}_{A_1B_2}$ unsteerable (no-way steering), as demonstrated by the blue curves. When we take $p>1/2$ such as $p=0.7$, the input state $\rho_{A_1B_1}$ becomes steerable, giving rise to one-way or two-way steering for the output state $\rho^{\text{out}}_{A_1B_2}$ (see the red curves). This suggests that both one-way and two-way steering can be obtained by tuning the measurement parameter θ_1 for a definite steerable input state $\rho_{A_1B_1}$. Moreover, we find that the optimal steerability of the output state $\rho^{\text{out}}_{A_1B_2}$ can be achieved under an optimal measurement $M(\theta_1^{\text{opt}})$ (see green stars in figures 2(b) and (c)), where

$$\theta_1^{\text{opt}}=\frac{\pi}{2}-\beta_2. \tag{9}$$

The optimal measurement yields the same output state as the input state $\rho_{A_1B_1}$. This implies that the steerable input state can be perfectly transferred to the output state with the optimal measurement. From figure 2(a), one can see that one-way and two-way steering for the output state can also be attained by tuning the parameter β_2 with the fixed θ_1, which is consistent with g_2 given by equation (8).

3.2. Three entangled sources

In the following, we expand the network to the case of $N=3$. In this scenario, the input state can be considered not only as the product of three individual entangled sources but also as the product state of the third entangled source and the output state of the first two entangled sources. Clearly, these two perspectives are equivalent. However, from the latter perspective, the scenario for $N=3$ can be directly reduced to that of $N=2$, except for the inclusion of an additional measurement $M(\theta_2)$ on parties B_2 and A_3 and the introduction of a variable parameter β_3. This results in a network comprising three entangled sources that are more adjustable. Following the procedure in appendix A, the output state of the network can be expressed as

$$\rho^{\text{out}}_{A_1B_3} = p\psi_{A_1B_3} + (1-p)\frac{I_{A_1}}{2}\otimes\psi_{B_3}, \tag{10}$$

where $\psi_{A_1B_3} = |g_3\rangle_{A_1B_3}\langle g_3|$ and $\psi_{B_3} = \text{Tr}_{A_1}(\psi_{A_1B_3})$. The g-function is

$$g_3 = \frac{1}{2}\arccos\left(1 - \frac{2}{1+\prod_{j=1}^{2}\cot^2\theta_j\cot^2\beta_{j+1}}\right). \tag{11}$$

Apparently, the steerability of the output state $\rho^{\text{out}}_{A_1B_3}$ from A_1 to B_3 is $R_{A_1\to B_3} = (2p)^{-1}$, which is the same as $R_{A_1\to B_2}$ because of their similar forms. This indicates that the steerability from A_1 to B_1 of the input state $\rho_{A_1B_1}$ can be perfectly transferred to the steerability from A_1 to B_3 of the output state $\rho^{\text{out}}_{A_1B_3}$. For the backward steering from B_3 to A_1, we find that its pattern, as functions of θ_1 and θ_2 in figure 3, displays four-leaf clovers with *adjustable* symmetry (see the dashed box) by tuning the parameter β ($\beta_2=\beta_3=\beta$ are assumed) for fixed p, which is different from the case of $N=2$. Specifically, when $\beta=\pi/4$, the second and third entangled sources are in an symmetric state, i.e. Bell state, giving rise to symmetric pattern similar to the case of $N=2$ (see figures 3(b) and (e)). But when $\beta=\pi/6$ or $\pi/3$, the steeribility of the output state from B_3 to A_1 only keeps axial-, rotational-, and central-symmetry, while the translation-symmetry is broken (see figures 3 (a)–(f)). This is because that the second and third entangled sources are in the unsymmetric Bell-like state in the cases of $\beta\neq(2k+1)\pi/4$ $(k=0,1,2,\ldots)$. In addition, we find that neighboring leafs for a four-leaf clover along θ_2-(θ_1-) direction exhibit repulsion (attraction) from each other for $\beta=\pi/6$ (see figures 3(a) and (d)). But when $\beta=\pi/3$, the situation is fully reversed (see figures 3(c) and (f)). It is evident that a larger value of p results in both a larger steering zone and a larger optimal value by comparing the first and second panels. This is because the input state described by equation (5) approaches the Bell state more closely as p increases. From figure 3, we further confirm that optimal backward steering can be periodically predicted at

$$\theta_1^{\text{opt}} = \pi/2-\beta_2 \quad \text{and} \quad \theta_2^{\text{opt}} = \pi/2-\beta_3. \tag{12}$$

The periodicity can also be roughly predicted from g-function given by equation (11). As the backward steering can be tuned from zero to its optimal value, so one-way and two-way steering of the output state can be achieved in a controlled manner.

3.3. Multiple entangled sources

In this part, we further consider that the network is extended to the case of N-pair entangled sources, where the first source is in a Werner state and each of the rest is in a Bell-like state. By utilizing the inductive method based on the cases of $N=2$ and 3, the output state can be written as

$$\rho^{\text{out}}_{A_1B_N} = p\psi_{A_1B_N} + (1-p)\frac{I_{A_1}}{2}\otimes\psi_{B_N}, \tag{13}$$

where $\psi_{A_1B_N} = |g_N\rangle_{A_1B_N}\langle g_N|$ with $|g_N\rangle_{A_1B_N} = \cos g_N|00\rangle_{A_1B_N} + \sin g_N|11\rangle_{A_1B_N}$, and $\psi_{B_N} = \text{Tr}_{A_1}(\psi_{A_1B_N})$. The g-function here is given by

$$g_N = \frac{1}{2}\arccos\left(1 - \frac{2}{1+\prod_{j=1}^{N-1}\cot^2\theta_j\cot^2\beta_{j+1}}\right). \tag{14}$$

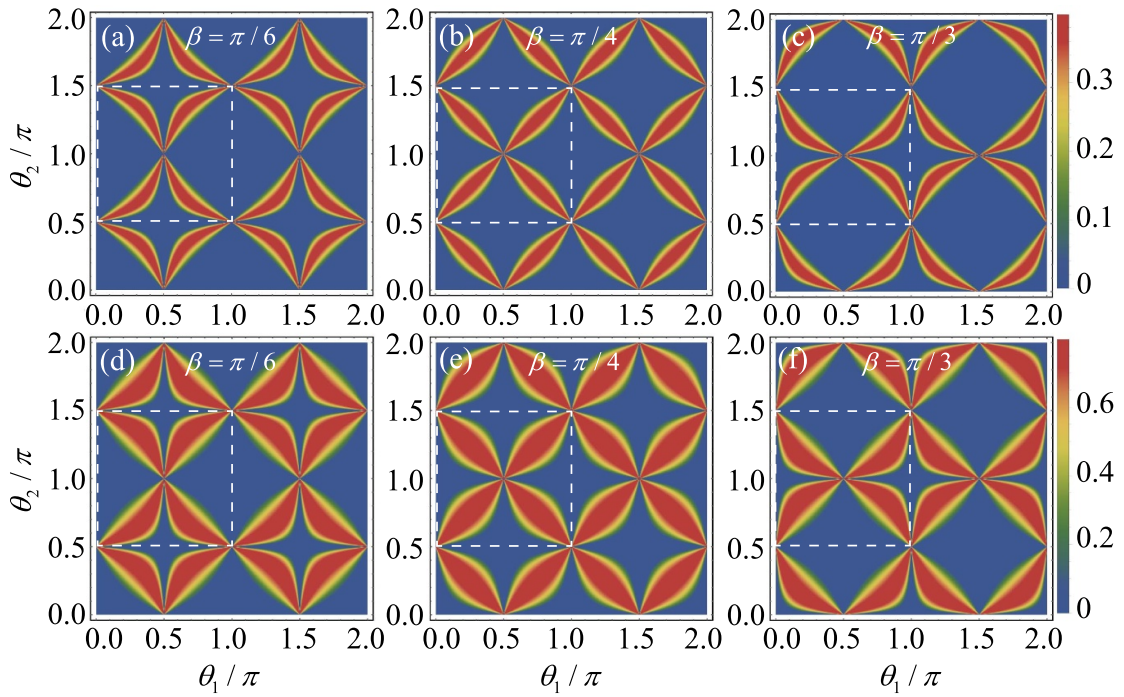

Figure 3. Backward steering ($\mathcal{R}_{B_3\to A_1}$) in a 3-pair entangled sources network versus the measurement parameters θ_1 and θ_2 with (a), (d) $\beta=\pi/6$, (b), (e) $\beta=\pi/4$, and (c), (f) $\beta=\pi/6$, where $p=0.7$ and $p=0.9$ are respectively taken in the upper and lower panels.

According to the results in the cases of $N=2$ and $N=3$, the critical radius of the output state $\rho^{\text{out}}_{A_1B_N}$ from A_1 to B_N is $R_{A_1\to B_N}=(2p)^{-1}=R_{A_1\to B_1}$. This indicates that the steerability from A_1 to B_1 can always be perfectly transferred to the steerability from A_1 to B_N, regardless of the number of intermediate parties and the measurement. However, for the backward steering from B_N to A_1, its critical radius $R_{B_N\to A_1}$ is severely affected by the unoptimal measurement number. These two situations are numerically shown in figure 4(a), respectively, denoted by red circles and squares. The corresponding parameters are $p=0.9$, $\beta=\beta_2=\ldots=\beta_N=\pi/6$, and $\theta=\theta_1=\theta_2=\ldots=\theta_{N-1}$. Apparently, the backward steering decreases with increasing measurement number. With the parameter $\theta=\pi/6$ adopted in figure 4(a), one can see that $\mathcal{R}_{B_N\to A_1}=0$ when $N=3$. This means that the output state $\rho^{\text{out}}_{A_1B_N}$ is two-way (one-way) steering when $N<3$ ($N\geqslant 3$). For a more complicated network, more measurements ($N\geqslant 4$) are required for achieving one (two)-way steering between two remote parties (A_1 and B_N). This can be realized by tuning measurement parameters in proximity to the optimal value, i.e.

$$\theta_j^{\text{opt}}=\frac{\pi}{2}-\beta_{j+1}\ \text{ with }\ j=1,2,\ldots,N-1, \tag{15}$$

as demonstrated by blue ($\theta=\pi/4$) and green ($\theta=5\pi/17$) markers in figures 4(b) and (c), where the optimal value $\theta^{\text{opt}}=\pi/3$ because of $\beta=\pi/6$.

In practice, optimal measurements cannot be made accurately. Therefore, the error (δ) between actual measurements (θ^{act}) and the optimal measurements (θ^{opt}) must be taken into account, which can be defined as

$$\delta=\theta^{\text{act}}/\theta^{\text{opt}}-1. \tag{16}$$

In figure 4(d), we plot the backward steering ($\mathcal{R}_{B_N\to A_1}$) versus the measurement error with different measurement number N, where $p=0.7$ and $\beta=\pi/6$. Clearly, $\mathcal{R}_{B_N\to A_1}$ can present with a larger error when the measurements are fewer, such as $N=5$ (see the black curve). By gradually adding the number of measurements, for example, from $N=10$ to $N=40$, the smaller and smaller error is allowed for non-vanishing backward steering. These indicate that as the number of measurements increases, the critical measurement error corresponding to the disappearance of the backward steering becomes smaller. In other words, the realization of two-way (one-way) steering in a many-body network requires measurements close to (away from) the optimal points when other parameters are fixed.

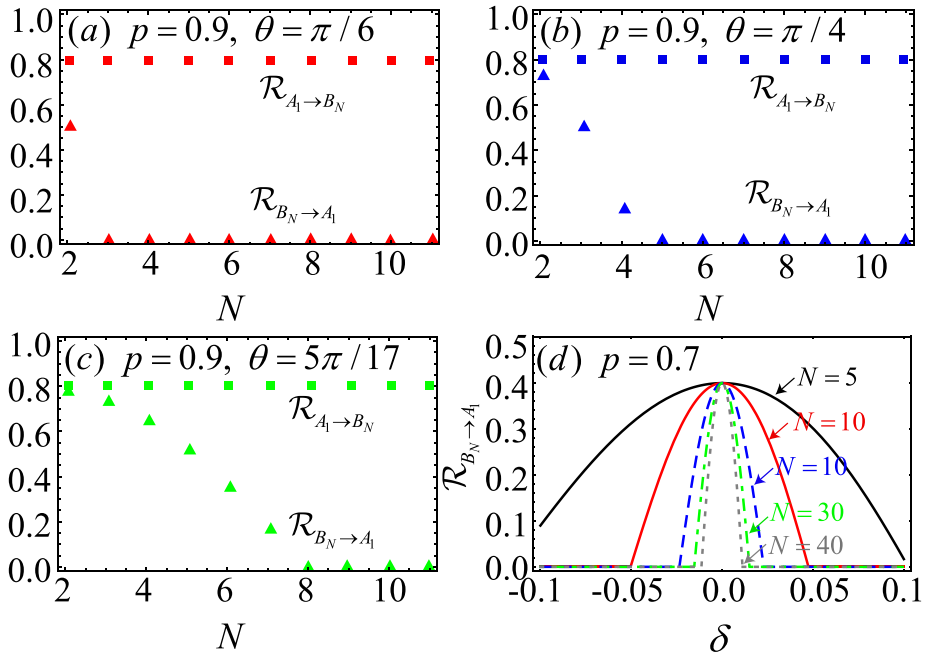

Figure 4. Forward ($\mathcal{R}_{A_1\to B_N}$) and backward steering ($\mathcal{R}_{B_N\to A_1}$) in a N-pair entangled sources network versus the measurement number N with (a) $\theta=\pi/6$, (b) $\pi/4$ and (c) $5\pi/17$. In (a)–(c), we take $p=0.9$. (d) Backward steering ($\mathcal{R}_{B_N\to A_1}$) as a function of the measurement error δ with different measurement number, where $p=0.7$. In (a)–(d), $\beta=\pi/6$ is used.

4. Conclusion

In summary, we propose a promising way to realize one-way and two-way steering between two remote parties (A_1 and B_N) in a linear quantum network by performing the joint measurements $\{M(\theta_j)\}_{j=1}^{N-1}$ on all intermediate parties. In our scheme, the reason for choosing the Werner state as the first entangled source is that: (1) the forward steering is the same as the backward steering; (2) after performing the joint measurements, the output state of the quantum network has a certain regularity, which can be obtained for the case of $N\geqslant 4$ through mathematical induction. By using the necessary and sufficient criterion (i.e. the critical radius), we find that the forward steering can always be perfectly transferred from the first entangled source to two endpoints, regardless of the number of the intermediate parties and the measurements. For the backward steering, its pattern behaves like a four-leaf clovers with rich symmetries, which is dependence of the input state of the network. With increasing the number of measurements, this means that the quantum network is formed by N ($N\geqslant 4$) entangled sources and $N-1$ joint measurements. We can show that not only the translation-symmetry of the pattern is broken, but also one-way and two-way steering can be obtained by tuning measurement parameters. We also consider the impact of the measurement error on the backward steering. Our work paves the way for a potential way to build the one-way and two-way steering with multiple measurements within the directional network.

Data availability statement

All data that support the findings of this study are included within the article (and any supplementary files).

Acknowledgments

This work was supported by the National Natural Science Foundation of China under Grant No. 12175001, the Open Foundation of Key Laboratory of Functional Materials and Devices for Informatics of Anhui Higher Education Institutes under Grant No. FMDI202412, the 'Pioneer' and 'Leading Goose' R & D Program of Zhejiang (Grant No. 2025C01028), the Natural Science Foundation of Zhejiang Province (Grant No. LY24A040004), and the Shenzhen International Quantum Academy (Grant No. SIQA2024KFKT010).

Appendix A. The derivation of the output state in equation (7)

For the case of $N=2$, we take the product of an entangled Werner state $\rho_{A_1B_1}$ and an entangled pure state $\rho_{A_2B_2}$ as the input state. By performing the measurement $M(\theta_1)$ and tracing out the untrusted parties B_1 and A_2, the unnormalized output state can be expressed as

$$\begin{aligned}\sigma_{A_1B_2}^{\text{out}} &= \text{Tr}_{B_1A_2}\left[\rho_{A_1B_1}\otimes\rho_{A_2B_2}M(\theta_1)\right]\\ &= p\phi_{A_1B_2}+(1-p)\frac{I_{A_1}}{2}\otimes\sigma_{B_2},\end{aligned}\tag{A.1}$$

where

$$\begin{aligned}\phi_{A_1B_2} &= \text{Tr}_{B_1A_2}\left[|\text{Bell}\rangle_{A_1B_1}\langle\text{Bell}|\otimes\rho_{A_2B_2}M(\theta_1)\right],\\ \sigma_{B_2} &= \text{Tr}_{B_1A_2}\left[\frac{I_{B_1}}{2}\otimes\rho_{A_2B_2}M(\theta_1)\right].\end{aligned}\tag{A.2}$$

As the measurement $M(\theta_1)$ is performed on the untrusted parties B_1 and A_2, so $\sigma_{B_2}=\text{Tr}_{A_1}\left[\phi_{A_1B_2}\right]\equiv\phi_{B_2}$. Thus, $\sigma_{A_1B_2}^{\text{out}}$ in equation (A.1) reduces to

$$\sigma_{A_1B_2}^{\text{out}} = p\phi_{A_1B_2}+(1-p)\frac{I_{A_1}}{2}\otimes\phi_{B_2}.\tag{A.3}$$

We then go to establish the specific form of the state $\phi_{A_1B_2}$ in equation (A.3). For this, the following four measurement basis for parties B_1 and A_2 are employed,

$$\begin{aligned}|\psi_1\rangle_{B_1A_2} &= \cos\theta_1|00\rangle_{B_1A_2}+\sin\theta_1|11\rangle_{B_1A_2},\\ |\psi_2\rangle_{B_1A_2} &= \sin\theta_1|00\rangle_{B_1A_2}-\cos\theta_1|11\rangle_{B_1A_2},\\ |\psi_3\rangle_{B_1A_2} &= \cos\theta_1|01\rangle_{B_1A_2}+\sin\theta_1|10\rangle_{B_1A_2},\\ |\psi_4\rangle_{B_1A_2} &= \sin\theta_1|01\rangle_{B_1A_2}-\cos\theta_1|10\rangle_{B_1A_2},\end{aligned}\tag{A.4}$$

or equivalently,

$$\begin{aligned}|00\rangle_{B_1A_2} &= \cos\theta_1|\psi_1\rangle_{B_1A_2}+\sin\theta_1|\psi_2\rangle_{B_1A_2},\\ |11\rangle_{B_1A_2} &= \sin\theta_1|\psi_1\rangle_{B_1A_2}-\cos\theta_1|\psi_2\rangle_{B_1A_2},\\ |01\rangle_{B_1A_2} &= \cos\theta_1|\psi_3\rangle_{B_1A_2}+\sin\theta_1|\psi_4\rangle_{B_1A_2},\\ |10\rangle_{B_1A_2} &= \sin\theta_1|\psi_3\rangle_{B_1A_2}-\cos\theta_1|\psi_4\rangle_{B_1A_2}.\end{aligned}\tag{A.5}$$

With these basis, we have

$$\begin{aligned}|\text{Bell}\rangle_{A_1B_1}\otimes|\beta_2\rangle_{A_2B_2} &= |\phi_1\rangle_{A_1B_2}\otimes|\psi_1\rangle_{B_1A_2}+|\phi_2\rangle_{A_1B_2}\otimes|\psi_2\rangle_{B_1A_2}\\ &\quad+|\phi_3\rangle_{A_1B_2}\otimes|\psi_3\rangle_{B_1A_2}+|\phi_4\rangle_{A_1B_2}\otimes|\psi_4\rangle_{B_1A_2},\end{aligned}\tag{A.6}$$

where

$$\begin{aligned}|\phi_1\rangle_{A_1B_2} &= \frac{1}{\sqrt{2}}\left(\cos\beta_2\cos\theta_1|00\rangle+\sin\beta_2\sin\theta_1|11\rangle\right)_{A_1B_2},\\ |\phi_2\rangle_{A_1B_2} &= \frac{1}{\sqrt{2}}\left(\cos\beta_2\sin\theta_1|00\rangle-\sin\beta_2\cos\theta_1|11\rangle\right)_{A_1B_2},\\ |\phi_3\rangle_{A_1B_2} &= \frac{1}{\sqrt{2}}\left(\sin\beta_2\cos\theta_1|01\rangle+\cos\beta_2\sin\theta_1|10\rangle\right)_{A_1B_2},\\ |\phi_4\rangle_{A_1B_2} &= \frac{1}{\sqrt{2}}\left(\sin\beta_2\sin\theta_1|01\rangle-\cos\beta_2\cos\theta_1|10\rangle\right)_{A_1B_2}.\end{aligned}$$

When $M(\theta_1)=|\theta\rangle_{B_1A_2}\langle\theta|=|\psi_1\rangle_{B_1A_2}\langle\psi_1|$ is applied to parties B_1 and A_2, the state in equation (A.6) collapses to $|\phi_1\rangle_{A_1B_2}\otimes|\psi_1\rangle_{B_1A_2}$. By tracing out B_1 and A_2, we have

$$\phi_{A_1B_2}=|\phi_1\rangle_{A_1B_2}\langle\phi_1|.\tag{A.7}$$

Once equation (A.7) is obtained, the output state $\rho^{\text{out}}_{A_1B_2}$ can be calculated following the normalization procedure, i.e.

$$\rho^{\text{out}}_{A_1B_2} = \frac{\sigma^{\text{out}}_{A_1B_2}}{\text{Tr}\left(\sigma^{\text{out}}_{A_1B_2}\right)} = p\psi_{A_1B_2} + (1-p)\frac{I_{A_1}}{2}\otimes\psi_{B_2}, \tag{A.8}$$

with

$$\begin{aligned}\psi_{A_1B_2} &= \frac{\phi_{A_1B_2}}{\text{Tr}\left(\phi_{A_1B_2}\right)} = |g_2\rangle_{A_1B_2}\langle g_2|,\\ \psi_{B_2} &= \frac{\phi_{B_2}}{\text{Tr}\left(\phi_{B_2}\right)} = \text{Tr}_{A_1}\left(\psi_{A_1B_2}\right),\\ |g_2\rangle_{A_1B_2} &= \cos g_2|00\rangle_{A_1B_2} + \sin g_2|11\rangle_{A_1B_2},\end{aligned} \tag{A.9}$$

where $g_2 = \frac{1}{2}\arccos\left(1 - \frac{2}{1+\cot^2\beta_2\cot^2\theta_1}\right)$ is the g-function.

Appendix B. The calculation of the critical radii for the output state in equation (13)

For the critical radius $R_{A_1\to B_N}$ of the state $\rho^{\text{out}}_{A_1B_N}$, it has the analytical solution. In order to obtain of the analytical solution, we first introduce one property of the critical radius [51].

Property—For an arbitrary two-qubit state ρ, consider a local reversible operation V_B, and apply this operation V_B to the original state to obtain a new state

$$\rho' = \frac{(I_A\otimes V_B)\,\rho(I_A\otimes V_B)^\dagger}{\text{Tr}\left[(I_A\otimes V_B)\,\rho(I_A\otimes V_B)^\dagger\right]}. \tag{B.1}$$

For these two states, their critical radii satisfy the relation $R_{A\to B}(\rho') = R_{A\to B}(\rho)$.

By using the property, we consider a local reversible operation $V_{B_N} = \left[\text{Tr}_{A_1}\left(\rho^{\text{out}}_{A_1B_N}\right)\right]^{-\frac{1}{2}}$, apply this operation to the output state $\rho^{\text{out}}_{A_1B_N}$ to obtain a new state

$$\rho'_{A_1B_N} = \frac{(I_{A_1}\otimes V_{B_N})\,\rho^{\text{out}}_{A_1B_N}(I_{A_1}\otimes V_{B_N})^\dagger}{\text{Tr}\left[(I_{A_1}\otimes V_{B_N})\,\rho^{\text{out}}_{A_1B_N}(I_{A_1}\otimes V_{B_N})^\dagger\right]}. \tag{B.2}$$

Through rigorous mathematical calculations, we find that this new state $\rho'_{A_1B_N}$ is a Werner state, and the same as for the first entangled source, which shows that the critical radius of the output state can be given by $R_{A_1\to B_N}\left(\rho^{\text{out}}_{A_1B_N}\right) = (2p)^{-1}$. Thus, the forward steering $\mathcal{R}_{A_1\to B_N} = \max\left\{0, R^{-1}_{A_1\to B_N} - 1\right\} = \max\{0, 2p-1\}$ is not affected by the performed joint-measurements $M(\theta_j) = |\theta_j\rangle_{B_jA_{j+1}}\langle\theta_j|$ with $j = 1,2,\ldots,N-1$.

For the critical radius $R_{B_N\to A_1}$ of the state $\rho^{\text{out}}_{A_1B_N}$, it has no analytical solution and can only be calculated numerically using the definition of the critical radius in equation (2). Due to the large amount of computation, we only consider three cases $p = 0.5$, $p = 0.7$, $p = 0.9$ and use the Taylor series fitting method to obtain the approximate expression of the negative power of the critical radius.

When $p = 0.5$, its fitting function is

$$\begin{aligned}R^{-1}_{B_N\to A_1} = {}& 0.000\,524\,371 + 6.930\,72x + 3.003\,45x^2 - 134.205x^3\\ &+ 467.93x^4 - 800.941x^5 + 533.961x^6,\end{aligned} \tag{B.3}$$

when $p = 0.7$, its fitting function is

$$\begin{aligned}R^{-1}_{B_N\to A_1} = {}& -0.004\,247\,23 + 12.0541x - 10.55x^2 - 215.743x^3\\ &+ 1023.3x^4 - 1938.13x^5 + 1292.08x^6,\end{aligned} \tag{B.4}$$

when $p = 0.9$, its fitting function is

$$\begin{aligned}R^{-1}_{B_N\to A_1} = {}& -0.041\,4525 + 29.5148x - 206.512x^2 + 821.949x^3\\ &- 1982.05x^4 + 2784.23x^5 - 1856.15x^6,\end{aligned} \tag{B.5}$$

where $x = g_N/\pi$. The fitting results are shown in following figure B1.

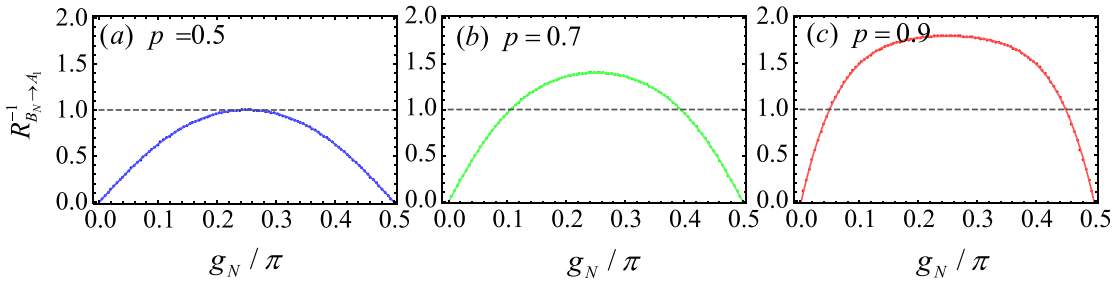

Figure B1. The results of the critical radius $R_{B_N \to A_1}$ varying with the function g_N are shown. The vertical axis represents $1/R_{B_N \to A_1}$, and the horizontal axis represents g_N/π. Figures (a), (b) and (c) respectively represent these three cases $p = 0.5$, $p = 0.7$, $p = 0.9$. In each subplot, uniformly choose 100 quantum states, and their critical radii are calculated using the definition of the critical radius. The 100 points in the figure reflect the variation of the critical radius with the function g_N. The solid lines represent the fitting results of these data points using the Taylor series fitting method. The upper part of the dashed line indicates that the quantum state is steerable from B_N to A_1, and the dashed line and its lower part indicate that the quantum state is unsteerable from B_N to A_1.

References

[1] Einstein A, Podolsky B and Rosen N 1935 Can quantum-mechanical description of physical reality be considered complete *Phys. Rev.* **47** 777
[2] Schrödinger E 1935 Discussion of relations between separated systems *Math. Proc. Camb. Phil. Soc.* **31** 555
[3] Wiseman H M, Jones S J and Doherty A C 2007 Steering, entanglement, nonlocality and the Einstein-Podolsky-Rosen paradox *Phys. Rev. Lett.* **98** 140402
[4] Quintino M T, Vértesi T, Cavalcanti D, Augusiak R, Demianowicz M, Acín A and Brunner N 2015 Inequivalence of entanglement, steering and Bell nonlocality for general measurements *Phys. Rev. A* **92** 032107
[5] Uola R, Costa A C S, Nguyen H C and Gühne O 2020 Quantum steering *Rev. Mod. Phys.* **92** 015001
[6] Horodecki R, Horodecki P, Horodecki M and Horodecki K 2009 Quantum entanglement *Rev. Mod. Phys.* **81** 865
[7] Chen J J, Fan X-G, Xiong W, Wang D and Ye L 2024 Nonreciprocal photon-phonon entanglement in Kerr-modified spinning cavity magnomechanics *Phys. Rev. A* **109** 043512
[8] Chen J J, Fan X-G, Xiong W, Wang D and Ye L 2023 Nonreciprocal entanglement in cavity-magnon optomechanics *Phys. Rev. B* **108** 024105
[9] Fan X-G, Sun W-Y, Ding Z-Y, Ming F, Yang H, Wang D and Ye L 2019 Universal complementarity between coherence and intrinsic concurrence for two-qubit states *New J. Phys.* **21** 093053
[10] Brunner N, Cavalcanti D, Pironio V S S, Scarani V and Wehner S 2014 Bell nonlocality *Rev. Mod. Phys.* **86** 419
[11] Zhong W X, Cheng G L and Hu X M 2017 One-way Einstein-Podolsky-Rosen steering via atomic coherence *Opt. Express* **25** 11584
[12] Händchen V, Eberle T, Steinlechner S, Samblowski A, Franz T, Werner R F and Schnabel R 2012 Observation of one-way Einstein-Podolsky-Rosen steering *Nat. Photon.* **6** 596
[13] Midgley S L W, Ferris A J and Olsen M K 2010 Asymmetric gaussian steering: when Alice and Bob disagree *Phys. Rev. A* **81** 022101
[14] Olsen M K 2013 Asymmetric Gaussian harmonic steering in second-harmonic generation *Phys. Rev. A* **88** 051802(R)
[15] Tischler N *et al* 2018 Conclusive experimental demonstration of one-way Einstein-Podolsky-Rosen steering *Phys. Rev. Lett.* **121** 100401
[16] Wollmann S, Walk N, Bennet A J, Wiseman H M and Pryde G J 2016 Observation of genuine one-way Einstein-Podolsky-Rosen steering *Phys. Rev. Lett.* **116** 160403
[17] Cavalcanti E G, He Q Y, Reid M D and Wiseman H M 2011 Unified criteria for multipartite quantum nonlocality *Phys. Rev. A* **84** 032115
[18] Gehring T, Händchen V, Duhme J, Furrer F, Franz T, Pacher C, Werner R F and Schnabel R 2015 Implementation of continuous-variable quantum key distribution with composable and one-sided-device-independent security against coherent attacks *Nat. Commun.* **6** 8795
[19] Walk N *et al* 2016 Experimental demonstration of Gaussian protocols for one-sided device-independent quantum key distribution *Optica* **3** 634
[20] Branciard C, Cavalcanti E G, Walborn S P, Scarani V and Wiseman H M 2012 One-sided device-independent quantum key distribution: security, feasibility and the connection with steering *Phys. Rev. A* **85** 010301(R)
[21] Acín A, Massar S and Pironio S 2012 Randomness versus nonlocality and entanglement *Phys. Rev. Lett.* **108** 100402
[22] Passaro E, Cavalcanti D, Skrzypczyk P and Acín A 2015 Optimal randomness certification in the quantum steering and prepare-and-measure scenarios *New J. Phys.* **17** 113010
[23] Skrzypczyk P and Cavalcanti D 2018 Maximal randomness generation from steering inequality violations using qudits *Phys. Rev. Lett.* **120** 260401
[24] Piani M and Watrous J 2009 All entangled states are useful for channel discrimination *Phys. Rev. Lett.* **102** 250501
[25] Piani M and Watrous J 2015 Necessary and sufficient quantum information characterization of Einstein-Podolsky-Rosen steering *Phys. Rev. Lett.* **114** 060404
[26] Cavalcanti D and Skrzypczyk P 2016 Quantitative relations between measurement incompatibility, quantum steering and nonlocality *Phys. Rev. A* **93** 052112
[27] Chen S-L, Budroni C, Liang Y-C and Chen Y-N 2016 Natural framework for device-independent quantification of quantum steerability, measurement incompatibility and self-testing *Phys. Rev. Lett.* **116** 240401
[28] He Q Y and Reid M D 2013 Genuine multipartite Einstein-Podolsky-Rosen steering *Phys. Rev. Lett.* **111** 250403
[29] Kogias I, Xiang Y, He Q and Adesso G 2017 Unconditional security of entanglement-based continuous-variable quantum secret sharing *Phys. Rev. A* **95** 012315

[30] Xiang Y, Kogias I, Adesso G and He Q 2017 Multipartite Gaussian steering: monogamy constraints and quantum cryptography applications *Phys. Rev. A* **95** 010101(R)
[31] Reid M D 2013 Signifying quantum benchmarks for qubit teleportation and secure quantum communication using Einstein-Podolsky-Rosen steering inequalities *Phys. Rev. A* **88** 062338
[32] He Q, Rosales-Zárate L, Adesso G and Reid M D 2015 Secure continuous variable teleportation and Einstein-Podolsky-Rosen steering *Phys. Rev. Lett.* **115** 180502
[33] Cavalcanti D, Skrzypczyk P and Šupić I 2017 All entangled states can demonstrate nonclassical teleportation *Phys. Rev. Lett.* **119** 110501
[34] Cavalcanti E G, Jones S J, Wiseman H M and Reid M D 2009 Experimental criteria for steering and the Einstein-Podolsky-Rosen paradox *Phys. Rev. A* **80** 032112
[35] Quan Q, Zhu H, Liu S-Y, Fei S-M, Fan H and Yang W-L 2016 Steering Bell-diagonal states *Sci. Rep.* **6** 22025
[36] Costa A C S and Angelo R M 2016 Quantification of Einstein-Podolsky-Rosen steering for two-qubit states *Phys. Rev. A* **93** 020103(R)
[37] Fan X G, Yang H, Ming F, Wang D and Ye L 2021 Constraint relation between steerability and concurrence for two-qubit states *Ann. Phys., Lpz.* **533** 2100098
[38] Saunders D J, Jones S J, Wiseman H M and Pryde G J 2010 Experimental EPR-steering using Bell-local states *Nat. Phys.* **6** 845
[39] Fan X-G, Zhao F, Yang H, Ding Z-Y, Wang D and Ye L 2023 Optimized steering criterion based on infinity measurements for two-qubit states *Opt. Express* **31** 16719
[40] Bartkiewicz K, Lemr K, Černoch A and Miranowicz A 2017 Bell nonlocality and fully entangled fraction measured in an entanglement-swapping device without quantum state tomography *Phys. Rev. A* **95** 030102
[41] Schneeloch J, Broadbent C J, Walborn S P, Cavalcanti E G and Howell J C 2013 Einstein-Podolsky-Rosen steering inequalities from entropic uncertainty relations *Phys. Rev. A* **87** 062103
[42] Kriváchy T, Fröwis F and Brunner N 2018 Tight steering inequalities from generalized entropic uncertainty relations *Phys. Rev. A* **98** 062111
[43] Costa A C S, Uola R and Gühne O 2018 Steering criteria from general entropic uncertainty relations *Phys. Rev. A* **98** 050104(R)
[44] Żukowski M, Dutta A and Yin Z 2015 Geometric Bell-like inequalities for steering *Phys. Rev. A* **91** 032107
[45] Lai L and Luo S 2022 Detecting Einstein-Podolsky-Rosen steering via correlation matrices *Phys. Rev. A* **106** 042402
[46] Skrzypczyk P, Navascués M and Cavalcanti D 2014 Quantifying Einstein-Podolsky-Rosen steering, Phys. Rev. Lett. **112** 180404
[47] Zeng Q 2022 One-way Einstein-Podolsky-Rosen steering beyond qubits *Phys. Rev. A* **106** 032202
[48] Xiao Y, Ye X-J, Sun K, Xu J-S, Li C-F and Guo G-C 2017 Demonstration of multisetting one-way Einstein-Podolsky-Rosen steering in two-qubit systems *Phys. Rev. Lett.* **118** 140404
[49] Sun K, Ye X-J, Xu J-S, Xu X-Y, Tang J-S, Wu Y-C, Chen J-L, Li C-F and Guo G-C 2016 Experimental quantification of asymmetric Einstein-Podolsky-Rosen steering *Phys. Rev. Lett.* **116** 160404
[50] Han X-H, Qu H-C, Fan X, Xiao Y and Gu Y-J 2022 Manipulating the quantum steering direction with sequential unsharp measurements *Phys. Rev. A* **106** 042416
[51] Nguyen H C, Nguyen H-V and Gühne O 2019 Geometry of Einstein-Podolsky-Rosen correlations *Phys. Rev. Lett.* **122** 240401
[52] Fan X-G, Zhao F, Yang H, Ding Z-Y, Wang D and Ye L 2023 Experimental detection of quantum steerability based on the critical radius in an all-optical system *Phys. Rev. A* **107** 012419
[53] Wehner S, Elkouss D and Hanson R 2018 Quantum internet: a vision for the road ahead *Science* **362** eaam9288
[54] Munro W J, Azuma K, Tamaki K and Nemoto K 2015 Inside quantum repeaters *IEEE J. Sel. Top. Quantum Electron.* **21** 78
[55] Chen Y-N, Chen S-L, Lambert N, Li C-M, Chen G-Y and Nori F 2013 Entanglement swapping and testing quantum steering into the past via collective decay *Phys. Rev. A* **88** 052320
[56] Kirby B T, Santra S, Malinovsky V S and Brodsky M 2016 Entanglement swapping of two arbitrarily degraded entangled states *Phys. Rev. A* **94** 012336
[57] Bergou J A, Fields D, Hillery M, Santra S and Malinovsky V S 2021 Average concurrence and entanglement swapping *Phys. Rev. A* **104** 022425
[58] Bej P, Ghosal A, Roy A, Mal S and Das D 2022 Creating quantum correlations in generalized entanglement swapping *Phys. Rev. A* **106** 022428
[59] Qi X, Zhai A and Yang L 2024 Quantum correlations in a chain-type quantum network *Commun. Theor. Phys.* **76** 065103
[60] Wang M, Qin Z and Su X 2017 Swapping of Gaussian Einstein-Podolsky-Rosen steering *Phys. Rev. A* **95** 052311
[61] Wang M, Qin Z, Wang X and Su X 2017 Einstein-Podolsky-Rosen-steering swapping between two Gaussian multipartite entangled states *Phys. Rev. A* **96** 022307
[62] Jones B D M, Šupić I, Uola R, Brunner N and Skrzypczyk P 2021 Network quantum steering, *Phys. Rev. Lett.* **127** 170405